Allele-specific knockouts reveal a role for *apontic-like* in the evolutionary loss of larval pigmentation in the domesticated silkworm, *Bombyx mori*

Kenta Tomihara[1*], Peter Andolfatto[2], Takashi Kiuchi[1*]

[1]Graduate School of Agricultural and Life Sciences, The University of Tokyo, Yayoi, Bunkyo-ku, Tokyo 113-8657, Japan

[2]Department of Biological Sciences, Columbia University, New York, NY 10026, USA

*Corresponding Author:

Kenta Tomihara: tomihara@g.ecc.u-tokyo.ac.jp

Takashi Kiuchi: kiuchi@g.ecc.u-tokyo.ac.jp

Running title: Genome editing in *Bombyx mandarina*

Abstract

The domesticated silkworm, *Bombyx mori*, and its wild progenitor, *B. mandarina*, are extensively studied as a model case of the evolutionary process of domestication. A conspicuous difference between these species is the dramatic reduction in pigmentation in both larval and adult *B. mori*. Here we evaluate the efficiency of CRISPR/Cas9-targeted knockouts of pigment-related genes as a tool to understand their potential contributions to domestication-associated pigmentation loss in *B. mori*. To demonstrate the efficacy of targeted knockouts in *B. mandarina*, we generated a homozygous CRISPR/Cas9-targeted knockout of *yellow-y*. In *yellow-y* knockout mutants, black body color became lighter throughout the larval, pupal and adult stages, confirming a role for this gene in pigment formation. Further, we performed *allele-specific* CRISPR/Cas9-targeted knockouts of the pigment-related transcription factor, *apontic-like* (*apt-like*) in *B. mori* × *B. mandarina* F_1 hybrid individuals. Knockout of the *B. mandarina* allele of *apt-like* in F_1 embryos results in depigmented patches on the dorsal integument of larvae, whereas corresponding knockouts of the *B. mori* allele consistently exhibit normal F_1 larval pigmentation. These results demonstrate a contribution of *apt-like* to the evolution of reduced pigmentation in *B. mori*. Together, our results demonstrate the feasibility of CRISPR/Cas9-targeted knockouts as a tool for understanding the genetic basis of traits associated with *B. mori* domestication.

Key words: *Bombyx mandarina*, domestication, pigmentation, CRISPR/Cas9, reciprocal hemizygosity test.

Brief abstract

Bombyx mori and its wild progenitor are an important model for the study of phenotypic evolution associated with domestication. As proof-of-principle, we used CRISPR/Cas9 to generate targeted knockouts of two pigmentation-related genes. By generating a homozygous knockout of *yellow-y* in *B. mandarina*, we confirmed this gene's role in pigment formation. Further, by generating *allele-specific* knockouts of *apontic-like* (*apt-like*) in *B. mori* × *B. mandarina* F_1 hybrids, we establish that evolution of *apt-like* contributed to reduced pigmentation during *B. mori* domestication.

Graphical TOC/Abstract

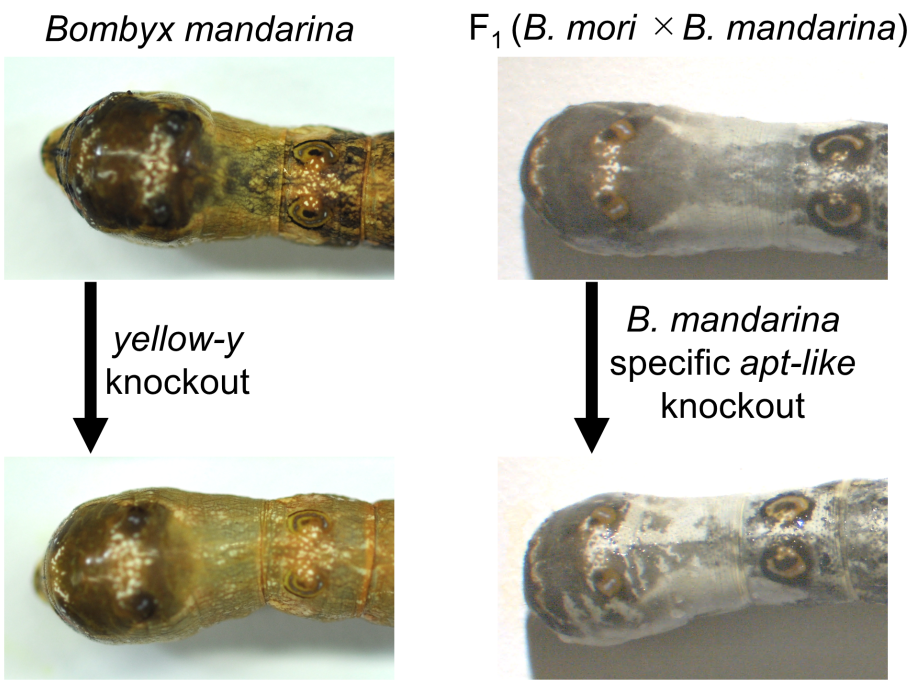

Introduction

The silkworm, *Bombyx mori*, was domesticated over 5000 years ago from its wild progenitor species, *B. mandarina*. Under long-term artificial selection, *B. mori* acquired various characteristics suitable for sericulture. For example, the weight of the cocoon shell of *B. mori* is much higher than that of *B. mandarina* (Ômura 1950, Li *et al.* 2017, Fang *et al.* 2020). In addition, *B. mori* moths lost their flying ability due to the degeneration of their flight muscles and a reduction in wing stiffness (Lu *et al.* 2020). Among the most conspicuous domestication-associated traits is a marked reduction in pigmentation in *B. mori* larvae and adults relative to *B. mandarina* (Figure 1A). Curiously, depigmentation is a major trait contributing to the so-called "domestication syndrome" observed in a variety of domesticated animals, but for reasons that are not well-understood (Wilkins *et al.* 2014).

The genetic basis of pigmentation loss associated with *B. mori* domestication is not yet known. Previous studies reported that melanin synthesis pathway genes *tyrosine hydroxylase* (*TH*) and *aspartate decarboxylase* (*ADC*, also known as *black*) were potentially targets of selection during silkworm domestication (Yu *et al.* 2011, Xiang *et al.* 2018). Pigmentation patterning genes are also likely to be associated with the body color differences between *B. mori* and *B. mandarina*. The wild-type *B. mori* larvae are largely white but exhibit melanic spots (*i.e.* eye spots, crescent spots and star spots, Figure 1A). *B. mandarina* larvae, on the other hand, are substantially darker, and exhibit extensive dorsal pigment patterning that includes banding and spots (Figure 1A).

In *B. mori*, distinct alleles of the genetic locus, *p*, encode at least 15 different larval markings such as spots, stripes, and banding (Yoda *et al.* 2014). The gene underlying allelic variation at *p*, *apontic-like* (*apt-like*), encodes a transcription factor that is likely to regulate the expression of melanin synthesis pathway genes such as *yellow-y*, *ebony*, *TH*, *Dopa decarboxylase* (*DDC*) and *laccase 2* (Futahashi *et al.* 2008, Yoda *et al.* 2014) (Figure 1B). While *apt-like* has been implicated in pigmentation differences among *B. mori* strains, it's potential role in depigmentation of *B. mori* during domestication is not known. A hybrid strain (semiconsomic T02), in which chromosome 2 of *B. mandarina* has been substituted into the genomic background of *B. mori*, exhibits a phenotype similar to that of the *B. mori* allele *moricaud* (p^M) (Fujii *et al.* 2021). Since *apt-like* resides on chromosome 2, dorsal pigmentation patterning on the larvae of *B. mandarina* that is absent in *B. mori* was hypothesized to be controlled by the expression of *apt-like* (Yoda *et al.* 2014, Fujii *et al.* 2021), although direct evidence is lacking.

The genetic analysis of domestication-associated loss of pigmentation in *B. mori* has been challenging because deficiencies in candidate genes can result in lethality. For example, in the fruit fly, *Drosophila melanogaster*, *TH*-deficient (*pale*) mutants die at embryonic stage (Neckameyer and White 1993). In *B. mori*, *TH*-deficient mutants (*sch lethal*, sch^l) and RNAi-mediated knockdowns of *TH* are both lethal at embryonic stage (Liu *et al.* 2010). In addition, *apt* mutants in *D. melanogaster* die at embryonic stage (Eulenberg and Schuh 1997, Gellon *et al.* 1997), and RNAi-mediated knockdown of *apt-like* in *B. mori* embryos results in death before hatching (Yoda *et al.* 2014).

93 The issue of lethality is likely to continue to impede the genetic analysis of
94 pigmentation loss and other domestication-associated traits in *B. mori*. Recently, several
95 candidate genes associated with domestication in *B. mori* have been identified using
96 quantitative trait locus (QTL) mapping, including silk production (Li *et al.* 2017, Fang
97 *et al.* 2020), larval climbing ability (Wang, Lin, *et al.* 2020), and mimicry (Wang, Lin,
98 *et al.* 2020). In addition, a recent population genetic analysis identified 300 candidate
99 genes as targets of recent selection in *B. mori*, some of which are likely to be associated
100 with silk production and voltinism (Xiang *et al.* 2018). Despite these efforts, reverse
101 genetic approaches such as targeted gene knockouts and editing (Takasu *et al.* 2010,
102 2013, Wang *et al.* 2013), gene silencing (Quan *et al.* 2002), or transgenesis (Tamura *et*
103 *al.* 2000) will likely be required to fully understand the function of these candidate genes
104 and their potential contribution to domestication-associated traits in *B. mori*. Notably,
105 the functions of domestication candidate genes have been tested by reverse genetics
106 approaches in *B. mori* (Xiang *et al.* 2018) but these approaches, to our knowledge, have
107 not yet been implemented in *B. mandarina*.
108 Here we use CRISPR/Cas9-targeted knockouts of two candidate pigmentation
109 genes in two distinct contexts. First, we demonstrate the feasibility of CRISPR/Cas9-
110 targeted knockouts in *B. mandarina* by generating a homozygous *yellow-y* knockout
111 strain. Next, to circumvent the lethal effects of knocking out a second candidate gene,
112 *apt-like*, we use *allele-specific* CRISPR/Cas9-targeted knockouts in *B. mori* × *B.*
113 *mandarina* F_1 hybrids. The latter experiment also comprises a test (the "reciprocal

hemizygosity test", Steinmetz *et al.* 2002, Stern 2014) of the contribution of *apt-like* evolution to the domestication-associated loss of pigmentation in *B. mori*.

Results and discussion

A CRISPR/Cas9-targeted knockout of *yellow-y* in *B. mandarina.*

To demonstrate the feasibility of CRISPR/Cas9-targeted knockouts in *B. mandarina*, we focused on known pigmentation-related genes. *TH* is among the most compelling candidate genes in the melanin synthesis pathway that seems likely to underlie domestication-associated loss of pigmentation in *B. mori* (Yu *et al.* 2011, Xiang *et al.* 2018). However, *TH* knockout mutants are predicted to be lethal (Neckameyer and White 1993, Liu *et al.* 2010), rendering them difficult to study. Thus, we decided to target *yellow-y* (Figure 1B), a melanin synthesis gene that is downstream of *TH* and functions in melanin synthesis in wide range of insects including *B. mori* and other Lepidoptera and is predicted to be non-essential (Futahashi *et al.* 2008, Zhang *et al.* 2017, Chen *et al.* 2018, Matsuoka and Monteiro 2018, Liu *et al.* 2020, Wang, Huang, *et al.* 2020, Han *et al.* 2021, Shirai *et al.* 2021). After confirming the coding sequence annotation (CDS) of the *B. mandarina yellow-y* gene, we designed a unique CRISPR-RNA (crRNA) target site in exon 2 (Figure 2A, Table S1).

In *B. mori*, CRISPR/Cas9-targeted genome editing requires microinjection into non-diapausing eggs (Kanda and Tamura 1994). We obtained non-diapausing eggs by rearing *B. mandarina* larvae under 16 h-light/8 h-dark conditions (Kobayashi 1990). We then injected a mixture of crRNA, trans-activating crRNA (tracrRNA), and Cas9 into

336 *B. mandarina* embryos. Among 16 hatched larvae (G_0 generation), nine grew to adult moths (Table 1). We crossed six G_0 adults with wild-type moths and obtained generation 1 (G_1) eggs. Using a heteroduplex mobility assay on the PCR products from G_1 embryos, we confirmed that mutations were introduced at the target site in five of the six G_1 broods (Table 1, Figure S1), showing that CRISPR/Cas9-induced mutations of *yellow-y* were heritable. We then crossed G_1 siblings with each other and obtained *yellow-y* homozygous knockout individuals carrying a five-nucleotide deletion followed by a single-nucleotide substitution (Figure 2B), which results in a frame-shift and premature stop codon. We designated this mutant allele *yellow-y*$^{\Delta 5}$ and used it for further analyses.

B. mandarina yellow-y$^{\Delta 5}$ homozygotes hatched normally and their development was comparable to that of wild-type individuals (Figure 3). In homozygous *yellow-y*$^{\Delta 5}$ neonate larvae, the larval integument and the head capsule are reddish brown instead of the normal black (Figure 3A) and in final instar larvae, spots and dorsal pigmentation patterns are lighter than that of the wild type (Figure 3B). Later in development, the pupal integument of homozygous *yellow-y*$^{\Delta 5}$ mutants exhibits reddish color instead of the normal black (Figure 3C), and the body and wing spot markings of *yellow-y*$^{\Delta 5}$ adult moths are lighter than that of wild-type (Figure 3D). Further, the phenotypes of heterozygous *+/yellow-y*$^{\Delta 5}$ individuals were comparable to that of wild type (data not shown). Together, these observations suggest that, as observed in *B. mori* (Futahashi *et al.* 2008), *yellow-y* is a non-essential gene contributing to melanin pigment synthesis in *B. mandarina* and loss-of-function is recessive.

158 Comparative data from other species suggests that *yellow-y* functions
159 differently among lepidopteran species. For example, while *yellow-y* loss-of-function is
160 also found to be recessive in several other lepidopteran species (Liu *et al.* 2020, Wang,
161 Huang, *et al.* 2020, Han *et al.* 2021, Shirai *et al.* 2021), it is dominant in the black
162 cutworm, *Agrotis ipsilon* (Chen *et al.* 2018). Further, unlike *Bombyx*, *yellow-y*
163 knockouts in *Agrotis* are susceptible to dehydration (Chen *et al.* 2018) and mutants in
164 *Spodoptera* exhibit defects in body development, copulation, oviposition, and
165 hatchability (Liu *et al.* 2020, Han *et al.* 2021, Shirai *et al.* 2021). These observations
166 suggest that although the function of *yellow-y* in melanin synthesis is conserved,
167 additional *yellow-y* functions might be diverged among lepidopteran species. *yellow*
168 genes are a rapidly evolving gene family, and loss or duplication of some *yellow* genes
169 have been observed in Lepidoptera (Chen *et al.* 2018, Liu *et al.* 2020, Han *et al.* 2021,
170 Shirai *et al.* 2021). It is possible that functions of *yellow-y* outside of melanin synthesis
171 in *Bombyx* are compensated for by other *yellow* paralogs. In Lepidoptera, the function
172 of most *yellow* genes remained unknown except for *yellow-y* (Futahashi *et al.* 2008,
173 Zhang *et al.* 2017, Chen *et al.* 2018, Matsuoka and Monteiro 2018, Liu *et al.* 2020, Wang,
174 Huang, *et al.* 2020, Han *et al.* 2021, Shirai *et al.* 2021), *yellow-e* (Ito *et al.* 2010), *yellow-*
175 *d* (Zhang *et al.* 2017) and *yellow-h2/3* (Zhang *et al.* 2017). Further studies of *yellow*
176 genes including *yellow-y* in diverse insect species are required to understand the
177 functions and evolution of *yellow* paralogs.

178 While our results demonstrate the feasibility of genome editing in *B. mandarina*,
179 these experiments are challenging due to low post-injection hatchability rates (4.8% in

our experiment). A recent study showed that the hatchability of *B. mandarina* eggs is generally lower than *B. mori* eggs, even under normal conditions (Zhu *et al.* 2019). To compare the hatchability of *B. mori* and *B. mandarina* embryos after injection, we injected three commonly used buffers (see Methods) and distilled water into embryos of both species and compared hatching rates. We found that the post-injection hatchability of *B. mandarina* embryos (0–8.3 %) is substantially lower than that of *B. mori* (22.9–62.5 %) in all experimental conditions (Table 2), suggesting that *B. mandarina* embryos are more sensitive to injection.

Allele-specific knockouts of _apt-like_ in interspecific F_1 hybrids.

Knockouts of some pigmentation pathway genes, such as *apt-like* and *TH*, are predicted to be lethal (Neckameyer and White 1993, Eulenberg and Schuh 1997, Gellon *et al.* 1997, Liu *et al.* 2010, Yoda *et al.* 2014). Considering this obstacle to the study of essential genes, together with the observation (above) of reduced hatchability of injected *B. mandarina* embryos, we instead opted for the alternative strategy of injecting *B. mori* × *B. mandarina* F_1 hybrids. Specifically, we conducted an *allele-specific* CRISPR/Cas9-targeted knockout of *apt-like* in F_1 embryos (from crosses between *B. mori* females and *B. mandarina* males). We reasoned that, because the components of these F_1 eggs is derived from the *B. mori* mother, these embryos should have post-injection hatchability similar to that of *B. mori*. We designed species-specific crRNA targeting *apt-like*, for which the targeted protospacer adjacent motif (PAM) sequence is only present in either *B. mori*- or *B. mandarina*-derived sequence (Methods, Figure 4, Table S1). For each

targeted allele, we injected a mixture of crRNA, tracrRNA and Cas9 into 48 F_1 embryos. To confirm that mutations were specifically introduced into the targeted allele, we extracted genomic DNA from adult legs and PCR-amplified the target sites. We then carried out heteroduplex mobility assays using a microchip electrophoresis system (Ota *et al.* 2013, Ansai *et al.* 2014), which show that various mutations were introduced into the *apt-like* target sequence in both of the *allele-specific* knockout series (Figure S2). The PCR products obtained from two representative individuals of each *allele-specific* knockout series were then cloned and sequenced (Figure 4). The sequences of cloned PCR products confirmed that various mutations were introduced into the target sites in both knockout series, some of which cause frameshifts and associated premature stop codons. All mutations detected in this experiment were specifically introduced only into the targeted allele.

In addition to spots, normal F_1 larvae have a dark body with darker greyish brown banding covering wide range of the dorsal surface, similar to the pattern for *B. mandarina* (Figure 1A, Figure S3). As predicted, post-injection hatchability of F_1 embryos was high whether targeting the *B. mori* (60%) or the *B. mandarina* (66%) allele. In the *apt-like* knockout series targeting the *B. mori* allele, all of the 26 larvae that survived to the fifth instar stage exhibited normal body color (Table 3, Figure 5). In contrast, for the *apt-like* knockout series targeting the *B. mandarina* allele, 24 of the 29 larvae that survived to the fifth instar stage exhibited white patches on dorsal pigmentation pattern banding that varied in size (Table 3, Figure 5, Figure S4). This result establishes a role for *apt-like* in body pigment formation and that the *B.*

224 *mandarina*-derived *apt-like* allele is dominant with respect to this trait. Notably,
225 however, the pigmentation of F_1 pupae and adult stages of the knockout series targeting
226 the *B. mori* or the *B. mandarina* allele both exhibited normal body color (data not shown).
227 Additionally, larval spots, which are also predicted to be controlled by *apt-like* (Yoda *et*
228 *al.* 2014), were also not affected the F_1 series targeting either the *B. mori* or the *B.*
229 *mandarina* allele (Figure 5, Figure S4). Since both wild-type ($+^p$) *B. mori* and *B.*
230 *mandarina* larvae exhibit spots (Figure 1A), we conclude that the *B. mori* or the *B.*
231 *mandarina*-derived *apt-like* alleles are both sufficient to direct the formation of larval
232 spots.

233 Our results have implications beyond merely confirming a role for *apt-like* in
234 *B. mandarina* larval pigmentation. The *allele-specific* knockouts of *apt-like* in F_1 hybrids
235 allows us to compare the phenotype of genetically identical hybrids that differ only at
236 the target locus (a framework called the "reciprocal hemizygosity test", Steinmetz *et al.*
237 2002, Stern 2014). As such, we can attribute the loss of pigmentation in the series
238 targeting the *B. mandarina* allele to evolution at the *apt-like* gene in *B. mori,* rather than
239 exclusively at a *trans*-acting factor. The Apt-like proteins of *B. mori* (p50T) and *B.*
240 *mandarina* (Sakado) differ by only one amino acid substitution: Alanine to Valine at
241 residue 188 (see DDBJ accession numbers LC706749 and LC706750). However, this
242 substitution is not observed in *B. mandarina* collected at different locations (see NCBI
243 accession numbers SRR6111377, SRR6111379, SRR6111381 and SRR6111382),
244 suggesting this is not a fixed amino acid difference between species. This implies that

245 evolution of an *apt-like cis*-regulatory element contributes to the observed phenotypic
246 difference between species.
247
248 **Conclusion**
249 Here we demonstrate the utility of CRISPR/cas9 genome editing in *B.*
250 *mandarina* and *B. mori* × *B. mandarina* F_1 hybrids to the study the function and
251 evolution of domestication-associated candidate genes. Focusing on two pigmentation-
252 related genes, we show that *apt-like* plays a role in larval body pigmentation patterning
253 (Figure 5), whereas *yellow-y* plays a more general role in pigmentation that is not pattern
254 dependent or specific to developmental life-stage (Figure 3B). These results are
255 consistent with the proposed roles of Apt-like as a transcription factor responsible for
256 larval color patterning, and Yellow-y as an enzyme in the melanin synthesis pathway
257 under control of Apt-like (Futahashi *et al.* 2008, Yoda *et al.* 2014). Further, using the
258 framework of the reciprocal hemizygosity test, we show that *apt-like* has evolved in *B.*
259 *mori* in a way that has specifically reduced larval body pigmentation, without affecting
260 the formation of larval spots or adult body pigmentation.
261 Despite being a powerful tool to study gene function and evolution, the *allele-*
262 *specific* knockout approach has several limitations. First, it requires sequence variants
263 distinguishing the parents of the F_1 hybrid that result in a PAM-site that is only present
264 in one of two species, limiting the potential to design *allele-specific* targets. However,
265 this limitation may be overcome by using Cas proteins that recognize different PAM-
266 sites (Leenay and Beisel 2017). For example, while the *Streptococcus pyogenes* Cas9

(*Sp*Cas9) protein has been used here, the Cas12a, which recognizes a distinct PAM sequence, has also been implemented in *B. mori* (Dong *et al.* 2020). In addition, recent studies have reported that *Sp*Cas9 can be modified to recognize alternative PAM sequences (Kleinstiver *et al.* 2015, 2016). A second limitation is that, given the mosacism of knockouts in G_0 individuals, one cannot exclude the possibility of false-negative phenotyping results. The cleavage efficiency of the CRISPR/Cas9 system is affected by several features, such as the sequences of PAM-distal and PAM-proximal regions of the guide RNA, the genomic context of the targeted DNA, as well as GC-content and secondary structure of the guide RNA (Liu *et al.* 2016). To minimize this problem, one can screen a large number of G_0 individuals and confirm that mutations were introduced with high efficiency (as in Figure 4 and Figure S2).

Despite these limitations, our results highlight several advantages of *allele-specific* knockouts in the F_1 over knockouts in *B. mandarina*. First, our results show that *B. mori* (female) × *B. mandarina* (male) F_1 embryos are substantially more tolerant to injection compared to *B. mandarina*. Second, *allele-specific* knockouts in the F_1 permit the study of essential genes (such as *apt-like*) at which knockouts are expected to be homozygous lethal and recessive with respect to the phenotype. Finally, *allele-specific* CRISPR/Cas9-targeted knockouts in F_1 hybrids have the added utility of identifying loci that have diverged in function between *B. mori* and *B. mandarina*, and contributing to domestication-related traits in *B. mori* using the framework of the reciprocal hemizygosity test. Thus, our study showcases the multifaceted utility of *allele-specific* knockouts in F_1 hybrids in the study of gene function and evolution.

Experimental procedures

Insects

The *B. mori* strain p50T, a single-paired descendant of individuals of strain p50 (a derivative from Daizo; https://shigen.nig.ac.jp/silkwormbase/ViewStrainDetail.do?name=p50), is maintained at our laboratory. The *B. mandarina* strain, Sakado, was originally collected in Sakado-city, Saitama, Japan, in 1982. Since then, it has been maintained at our laboratory by sib-mating. All larvae were reared on fresh mulberry leaves or artificial diet (SilkMate PS, NOSAN) under continuous 12 h-light/12 h-dark conditions at 25 °C with the exceptions described below. For injections in to *B. mandarina* embryos, we obtained non-diapausing eggs by rearing *B. mandarina* larvae under continuous long-day conditions (16 h-light/8 h-dark) at 25 °C (Kobayashi 1990). We then collected eggs in crosses between emerged adults. To generate *B. mori* × *B. mandarina* F_1 hybrid embryos for injection, we first incubated *B. mori* eggs at 15 ºC under continuous darkness (Kogure 1933). The hatched larvae were then reared under continuous 16 h-light/8 h-dark condition at 25 °C and females were crossed to *B. mandarina* males.

Confirmation of the *yellow-y* and *apt-like* coding sequences in *B. mandarina*.

Total RNA was extracted from the integument of fourth instar *B. mandarina* larvae using TRIzol (Thermo Fisher Scientific). Complementary DNA (cDNA) was reverse transcribed from total RNA using TaKaRa RNA PCR Kit (TaKaRa). Reverse transcriptase-PCR was performed using KOD One polymerase (TOYOBO). PCR

311 products were cloned into pGEM-T Easy Vector (Promega) and Sanger-sequenced
312 using the FASMAC sequencing service (Kanagawa, Japan).
313
314 **Knockout of *yellow-y* in *B. mandarina***
315 An unique crRNA target sequence in the *B. mori* genome was selected using
316 CRISPRdirect (https://crispr.dbcls.jp) (Table S1) (Naito *et al.* 2015). The uniqueness
317 of the target sequence in the *B. mandarina* genome was then confirmed by performing
318 blastn at SilkBase (http://silkbase.ab.a.u-tokyo.ac.jp). A mixture of crRNA, tracrRNA
319 and Cas9 Nuclease protein NLS (600 ng/μL; NIPPON GENE) in injection buffer (100
320 mM KOAc, 2 mM $Mg(OAc)_2$, 30 mM HEPES-KOH; pH 7.4) was injected into each
321 embryo within 3 h after oviposition (Yamaguchi *et al.* 2011).
322 The injected embryos (G_0 generation) were incubated at 25 °C in a humidified
323 Petri dish until hatching. Adult G_0 moths were crossed with wild-type *B. mandarina*,
324 and G_1 eggs were obtained. To detect heritable CRISPR/Cas9-induced mutations, ten
325 G_1 eggs were collected into one tube, and genomic DNA was prepared using the
326 HotSHOT method (Truett *et al.* 2000). The region containing the target site of *yellow-y*
327 crRNA was PCR-amplified using KOD One polymerase (TOYOBO). Mutations at the
328 target site were detected by heteroduplex mobility assay using the MultiNA microchip
329 electrophoresis system (SHIMAZU) with the DNA-500 reagent kit (Ota *et al.* 2013,
330 Ansai *et al.* 2014).
331 Adult G_1 moths from broods with heritable CRISPR/Cas9-induced mutations were
332 crossed with each other to obtain homozygous knockout mutants (G_2). To confirm

CRISPR/Cas9-induced mutations, we prepared genomic DNA, PCR-amplified the target region and detected mutations as described above using G_2 adult moths. To determine the precise nature of insertions, deletions and substitutions, PCR products obtained from G_2 individuals were directly Sanger-sequenced using the FASMAC sequencing service (Kanagawa, Japan).

Comparison of post-injection hatchability.

Three commonly used buffers (injection buffer 1 (Yamaguchi *et al.* 2011), injection buffer 2 (Tamura *et al.* 2000), PBS buffer) and distilled water into embryos of *B. mori* or *B. mandarina* within 3 h after oviposition. The injected embryos were incubated at 25 °C in a humidified Petri dish until hatching.

***Allele-specific* gene knockouts in F_1 hybrids.**

A PAM sequence is necessary for target recognition and following DNA cleavage in CRISPR/Cas system (Hsu *et al.* 2013, Anders *et al.* 2014), and *Sp*Cas9, which we used in this study, recognizes 5'-NGG-3' as PAM. We specifically targeted *Sp*Cas9 PAM-sites that differed in sequence between *B. mori* and *B. mandarina* (Figure 4, Table S1), allowing *allele-specific* DNA cleavage and gene knockout (Courtney *et al.* 2015, Christie *et al.* 2017). A mixture of crRNA, tracrRNA and Cas9 was injected to F_1 embryos as described above. To evaluate CRISPR/Cas9 cleavage efficiency, we extracted genomic DNA from G_0 adult legs and PCR-amplified the target region as

354 described above. PCR products were cloned into pGEM-T Easy Vector and Sanger-
355 sequenced using an ABI3130xl genetic analyzer (Applied Biosystems).
356

357 ## Acknowledgements

358 We are grateful to Katsuya Satta and Hisashi Tobita for assistance with the
359 experiments. We are also grateful to Professor Susumu Katsuma for helpful discussions.
360 We thank the Institute for Sustainable Agro-ecosystem Services, The University of
361 Tokyo, for facilitating the mulberry cultivation and the Biotron Facility at the
362 University of Tokyo for rearing the silkworms. This work was supported by JSPS
363 KAKENHI grant number JP20J22954 to KT and JP20H02997 to TK.
364

365 ## Data Availability

366 Full-length coding sequences of *B. mori yellow-y*, *B. mandarina yellow-y*, *B.*
367 *mori apt-like* and *B. mandarina apt-like* are available on the DDBJ under accession
368 numbers of LC706747, LC706748, LC706749 and LC706750, respectively.
369

370 ## Author contributions

371 KT, PA and TK designed the study. KT performed most of the experiments. KT
372 wrote the manuscript with intellectual input from TK and PA. All authors edited and
373 approved the final version of the manuscript and agree to be accountable for all aspects
374 of the work.
375

References

Anders, C., Niewoehner, O., Duerst, A., and Jinek, M., 2014. Structural basis of PAM-dependent target DNA recognition by the Cas9 endonuclease. *Nature*, 513 (7519), 569–573.

Ansai, S., Inohaya, K., Yoshiura, Y., Schartl, M., Uemura, N., Takahashi, R., and Kinoshita, M., 2014. Design, evaluation, and screening methods for efficient targeted mutagenesis with transcription activator-like effector nucleases in medaka. *Development, Growth & Differentiation*, 56 (1), 98–107.

Chen, X., Cao, Y., Zhan, S., Zhang, Y., Tan, A., and Huang, Y., 2018. Identification of *yellow* gene family in *Agrotis ipsilon* and functional analysis of *Aiyellow-y* by CRISPR/Cas9. *Insect Biochemistry and Molecular Biology*, 94, 1–9.

Christie, K.A., Courtney, D.G., DeDionisio, L.A., Shern, C.C., De Majumdar, S., Mairs, L.C., Nesbit, M.A., and Moore, C.B.T., 2017. Towards personalised allele-specific CRISPR gene editing to treat autosomal dominant disorders. *Scientific Reports*, 7 (1), 16174.

Courtney, D.G., Moore, J.E., Atkinson, S.D., Maurizi, E., Allen, E.H.A., Pedrioli, D.M.L., McLean, W.H.I., Nesbit, M.A., and Moore, C.B.T., 2015. CRISPR/Cas9 DNA cleavage at SNP-derived PAM enables both *in vitro* and *in vivo KRT12* mutation-specific targeting. *Gene Therapy*, 23 (1), 108–112.

Dong, Z., Qin, Q., Hu, Z., Zhang, X., Miao, J., Huang, L., Chen, P., Lu, C., and Pan, M., 2020. CRISPR/Cas12a mediated genome editing enhances *Bombyx mori* resistance to BmNPV. *Frontiers in Bioengineering and Biotechnology*, 8, 841.

398 Eulenberg, K.G. and Schuh, R., 1997. The tracheae defective gene encodes a bZIP
399 protein that controls tracheal cell movement during *Drosophila* embryogenesis.
400 *The EMBO Journal*, 16 (23), 7156–7165.
401 Fang, S., Zhou, Q., Yu, Q., and Zhang, Z., 2020. Genetic and genomic analysis for
402 cocoon yield traits in silkworm. *Scientific Reports*, 10 (1), 5682.
403 Fujii, T., Kiuchi, T., Daimon, T., Ito, K., Katsuma, S., Shimada, T., Yamamoto, K.,
404 and Banno, Y., 2021. Development of interspecific semiconsomic strains
405 between the domesticated silkworm, *Bombyx mori* and the wild silkworm, *B.*
406 *mandarina*. *Journal of Insect Biotechnology and Sericology*, 90 (2), 33–40.
407 Futahashi, R., Sato, J., Meng, Y., Okamoto, S., Daimon, T., Yamamoto, K., Suetsugu,
408 Y., Narukawa, J., Takahashi, H., Banno, Y., Katsuma, S., Shimada, T., Mita, K.,
409 and Fujiwara, H., 2008. *yellow* and *ebony* are the responsible genes for the larval
410 color mutants of the silkworm *Bombyx mori*. *Genetics*, 180 (4), 1995–2005.
411 Gellon, G., Harding, K.W., McGinnis, N., Martin, M.M., and McGinnis, W., 1997. A
412 genetic screen for modifiers of deformed homeotic function identifies novel
413 genes required for head development. *Development*, 124 (17), 3321–3331.
414 Han, W., Tang, F., Zhong, Y., Zhang, J., and Liu, Z., 2021. Identification of *yellow*
415 gene family and functional analysis of *Spodoptera frugiperda yellow-y* by
416 CRISPR/Cas9. *Pesticide Biochemistry and Physiology*, 178, 104937.
417 Hsu, P.D., Scott, D.A., Weinstein, J.A., Ran, F.A., Konermann, S., Agarwala, V., Li,
418 Y., Fine, E.J., Wu, X., Shalem, O., Cradick, T.J., Marraffini, L.A., Bao, G., and

419 Zhang, F., 2013. DNA targeting specificity of RNA-guided Cas9 nucleases.
420 *Nature Biotechnology*, 31 (9), 827–832.
421 Ito, K., Katsuma, S., Yamamoto, K., Kadono-Okuda, K., Mita, K., and Shimada, T.,
422 2010. Yellow-e determines the color pattern of larval head and tail spots of the
423 silkworm *Bombyx mori*. *Journal of Biological Chemistry*, 285 (8), 5624–5629.
424 Kanda, T. and Tamura, T., 1994. Microinjection method for DNA in early embryos of
425 the silkworm, *Bombyx mori*, using air-pressure. *Bulletin of the National Institute*
426 *of Sericultural and Entomological Science*, 2, 31-46 (in Japanese with English
427 summary).
428 Kleinstiver, B.P., Pattanayak, V., Prew, M.S., Tsai, S.Q., Nguyen, N.T., Zheng, Z.,
429 and Joung, J.K., 2016. High-fidelity CRISPR–Cas9 nucleases with no detectable
430 genome-wide off-target effects. *Nature*, 529 (7587), 490–495.
431 Kleinstiver, B.P., Prew, M.S., Tsai, S.Q., Topkar, V. V., Nguyen, N.T., Zheng, Z.,
432 Gonzales, A.P.W., Li, Z., Peterson, R.T., Yeh, J.-R.J., Aryee, M.J., and Joung,
433 J.K., 2015. Engineered CRISPR-Cas9 nucleases with altered PAM specificities.
434 *Nature*, 523 (7561), 481–485.
435 Kobayashi, J., 1990. Effects of photoperiod on the induction of egg diapause of
436 tropical races of the domestic silkworm, *Bombyx mori*, and the wild silkworm, *B.*
437 *mandarina*. *Japan Agricultural Research Quarterly*, 23 (3), 202–205.
438 Kogure, M., 1933. The influence of light and temperature on certain characters of the
439 silkworm, *Bombyx mori*. *Journal of the Faculty of Agriculture, Kyushu*
440 *University*, 4 (1), 1–93.

441 Leenay, R.T. and Beisel, C.L., 2017. Deciphering, communicating, and engineering
442 the CRISPR PAM. *Journal of Molecular Biology*, 429 (2), 177–191.
443 Li, C., Tong, X., Zuo, W., Luan, Y., Gao, R., Han, M., Xiong, G., Gai, T., Hu, H.,
444 Dai, F., and Lu, C., 2017. QTL analysis of cocoon shell weight identifies
445 *BmRPL18* associated with silk protein synthesis in silkworm by pooling
446 sequencing. *Scientific Reports*, 7 (1), 17985.
447 Liu, C., Yamamoto, K., Cheng, T.C., Kadono-Okuda, K., Narukawa, J., Liu, S.P.,
448 Han, Y., Futahashi, R., Kidokoro, K., Noda, H., Kobayashi, I., Tamura, T.,
449 Ohnuma, A., Banno, Y., Dai, F.Y., Xiang, Z.H., Goldsmith, M.R., Mita, K., and
450 Xia, Q.Y., 2010. Repression of *tyrosine hydroxylase* is responsible for the *sex-*
451 *linked chocolate* mutation of the silkworm, *Bombyx mori*. *Proceedings of the*
452 *National Academy of Sciences of the United States of America*, 107 (29), 12980–
453 12985.
454 Liu, X., Han, W., Ze, L., Peng, Y., Yang, Y., Zhang, J., Yan, Q., and Dong, S., 2020.
455 Clustered regularly interspaced short palindromic repeats/CRISPR-associated
456 protein 9 mediated knockout reveals functions of the *yellow-y* gene in
457 *Spodoptera litura*. *Frontiers in Physiology*, 11, 1643.
458 Liu, X., Homma, A., Sayadi, J., Yang, S., Ohashi, J., and Takumi, T., 2016. Sequence
459 features associated with the cleavage efficiency of CRISPR/Cas9 system.
460 *Scientific Reports*, 6 (1), 19675.
461 Lu, K., Liang, S., Han, M., Wu, C., Song, J., Li, C., Wu, S., He, S., Ren, J., Hu, H.,
462 Shen, J., Tong, X., and Dai, F., 2020. Flight muscle and wing mechanical

properties are involved in flightlessness of the domestic silkmoth, *Bombyx mori*. *Insects*, 11 (4), 220.

Matsuoka, Y. and Monteiro, A., 2018. Melanin pathway genes regulate color and morphology of butterfly wing scales. *Cell reports*, 24 (1), 56–65.

Naito, Y., Hino, K., Bono, H., and Ui-Tei, K., 2015. CRISPRdirect: software for designing CRISPR/Cas guide RNA with reduced off-target sites. *Bioinformatics*, 31 (7), 1120–1123.

Neckameyer, W.S. and White, K., 1993. *Drosophila* Tyrosine hydroxylase is encoded by the *pale* locus. *Journal of Neurogenetics*, 8 (4), 189–199.

Ômura, S., 1950. Researches on the behavior and ecological characteristics of the wild silkworm *Bombyx mandarina*. *Bulletin of the Imperial Sericultural Experiment Station*, 13 (3), 79-130 (in japanese with English summary).

Ota, S., Hisano, Y., Muraki, M., Hoshijima, K., Dahlem, T.J., Grunwald, D.J., Okada, Y., and Kawahara, A., 2013. Efficient identification of TALEN-mediated genome modifications using heteroduplex mobility assays. *Genes to Cells*, 18 (6), 450–458.

Quan, G.-X., Kim, I., Kômoto, N., Sezutsu, H., Ote, M., Shimada, T., Kanda, T., Mita, K., Kobayashi, M., and Tamura, T., 2002. Characterization of the kynurenine 3-monooxygenase gene corresponding to the *white egg 1* mutant in the silkworm *Bombyx mori*. *Molecular Genetics and Genomics*, 267 (1), 1–9.

483 Shirai, Y., Ohde, T., and Daimon, T., 2021. Functional conservation and
484 diversification of *yellow-y* in lepidopteran insects. *Insect Biochemistry and*
485 *Molecular Biology*, 128, 103515.
486 Steinmetz, L.M., Sinha, H., Richards, D.R., Spiegelman, J.I., Oefner, P.J., McCusker,
487 J.H., and Davis, R.W., 2002. Dissecting the architecture of a quantitative trait
488 locus in yeast. *Nature*, 416 (6878), 326–330.
489 Stern, D.L., 2014. Identification of loci that cause phenotypic variation in diverse
490 species with the reciprocal hemizygosity test. *Trends in Genetics*, 30 (12), 547–
491 554.
492 Takasu, Y., Kobayashi, I., Beumer, K., Uchino, K., Sezutsu, H., Sajwan, S., Carroll,
493 D., Tamura, T., and Zurovec, M., 2010. Targeted mutagenesis in the silkworm
494 *Bombyx mori* using zinc finger nuclease mRNA injection. *Insect Biochemistry*
495 *and Molecular Biology*, 40 (10), 759–765.
496 Takasu, Y., Sajwan, S., Daimon, T., Osanai-Futahashi, M., Uchino, K., Sezutsu, H.,
497 Tamura, T., and Zurovec, M., 2013. Efficient TALEN construction for *Bombyx*
498 *mori* gene targeting. *PLoS ONE*, 8 (9), e73458.
499 Tamura, T., Thibert, C., Royer, C., Kanda, T., Eappen, A., Kamba, M., Kômoto, N.,
500 Thomas, J.-L., Mauchamp, B., Chavancy, G., Shirk, P., Fraser, M., Prudhomme,
501 J.-C., and Couble, P., 2000. Germline transformation of the silkworm *Bombyx*
502 *mori* L. using a *piggyBac* transposon-derived vector. *Nature Biotechnology*, 18
503 (1), 81–84.

504 Truett, G.E., Heeger, P.S., Mynatt, R.L., Truett, A.A., Walker, J.A., and Warman,
505 M.L., 2000. Preparation of PCR-quality mouse genomic DNA with hot sodium
506 hydroxide and tris (HotSHOT). *Biotechniques*, 29 (1), 52–54.
507 Wang, M., Lin, Y., Zhou, S., Cui, Y., Feng, Q., Yan, W., and Xiang, H., 2020.
508 Genetic mapping of climbing and mimicry: two behavioral traits degraded
509 during silkworm domestication. *Frontiers in Genetics*, 11, 1568.
510 Wang, Y., Huang, Y., Xu, X., Liu, Z., Li, J., Zhan, X., Yang, G., You, M., and You,
511 S., 2020. CRISPR/Cas9-based functional analysis of *yellow* gene in the
512 diamondback moth, *Plutella xylostella*. *Insect Science*, 28 (5), 1504–1509.
513 Wang, Y., Li, Z., Xu, J., Zeng, B., Ling, L., You, L., Chen, Y., Huang, Y., and Tan,
514 A., 2013. The CRISPR/Cas System mediates efficient genome engineering in
515 *Bombyx mori*. *Cell Research*, 23 (12), 1414–1416.
516 Wilkins, A.S., Wrangham, R.W., and Tecumseh Fitch, W., 2014. The "domestication
517 syndrome" in mammals: a unified explanation based on neural crest cell
518 behavior and genetics. *Genetics*, 197 (3), 795–808.
519 Xiang, H., Liu, X., Li, M., Zhu, Y., Wang, L., Cui, Y., Liu, L., Fang, G., Qian, H.,
520 Xu, A., Wang, W., and Zhan, S., 2018. The evolutionary road from wild moth to
521 domestic silkworm. *Nature Ecology & Evolution*, 2 (8), 1268–1279.
522 Yamaguchi, J., Mizoguchi, T., and Fujiwara, H., 2011. siRNAs induce efficient RNAi
523 response in *Bombyx mori* embryos. *PLoS ONE*, 6 (9), e25469.

524 Yoda, S., Yamaguchi, J., Mita, K., Yamamoto, K., Banno, Y., Ando, T., Daimon, T.,
525 and Fujiwara, H., 2014. The transcription factor Apontic-like controls diverse
526 colouration pattern in caterpillars. *Nature Communications*, 5 (1), 4936.
527 Yu, H.-S., Shen, Y.-H., Yuan, G.-X., Hu, Y.-G., Xu, H.-E., Xiang, Z.-H., and Zhang,
528 Z., 2011. Evidence of selection at melanin synthesis pathway loci during
529 silkworm domestication. *Molecular Biology and Evolution*, 28 (6), 1785–1799.
530 Zhang, L., Martin, A., Perry, M.W., van der Burg, K.R.L., Matsuoka, Y., Monteiro,
531 A., and Reed, R.D., 2017. Genetic basis of melanin pigmentation in butterfly
532 wings. *Genetics*, 205 (4), 1537–1550.
533 Zhu, Y.N., Wang, L.Z., Li, C.C., Cui, Y., Wang, M., Lin, Y.J., Zhao, R.P., Wang, W.,
534 and Xiang, H., 2019. Artificial selection on storage protein 1 possibly
535 contributes to increase of hatchability during silkworm domestication. *PLOS*
536 *Genetics*, 15 (1), e1007616.
537
538
539

Figures and Tables

Table 1. Efficiency of CRISPR/Cas9-targeted knockout in *B. mandarina* targeting *yellow-y*.

# eggs injected	# hatched larvae	# adults	# G_1 broods	# G_1 broods carrying mutant alleles
336	16	9	6	5

546 **Table 2.** The hatchability of *B. mori* and *B. mandarina* embryos injected with an
547 injection buffer 1 (Yamaguchi *et al.* 2011), injection buffer 2 (Tamura *et al.* 2000), PBS
548 buffer and distilled water.

Treatment	Composition	*B. mori*		*B. mandarina*	
		# injected eggs	# hatched larvae	# injected eggs	# hatched larvae
Injection buffer 1	100 mM KOAc, 2 mM $Mg(OAc)_2$, 30 mM HEPES-KOH; pH 7.4	48	11	48	0
Injection buffer 2	0.5 mM phosphate buffer (pH 7.0), 5 mM KCl	48	30	48	4
PBS buffer	137 mM NaCl, 2.7 mM KCl, 10 mM Na_2HPO_4, 1.76mM KH_2PO_4; pH 7.4	48	23	48	1
Distilled water	–	48	17	48	2

549

550 **Table 3.** Efficiency of *allele-specific* knockouts of *apt-like* in F_1 hybrids.

Targeted allele	# eggs injected	# hatched larvae	# 5th instar larvae	# mosaic 5th instar larvae	# adults (male/female)
B. mori	48	29	26	0	26 (16/10)
B. mandarina	48	32	29	24	29 (18/11)

551

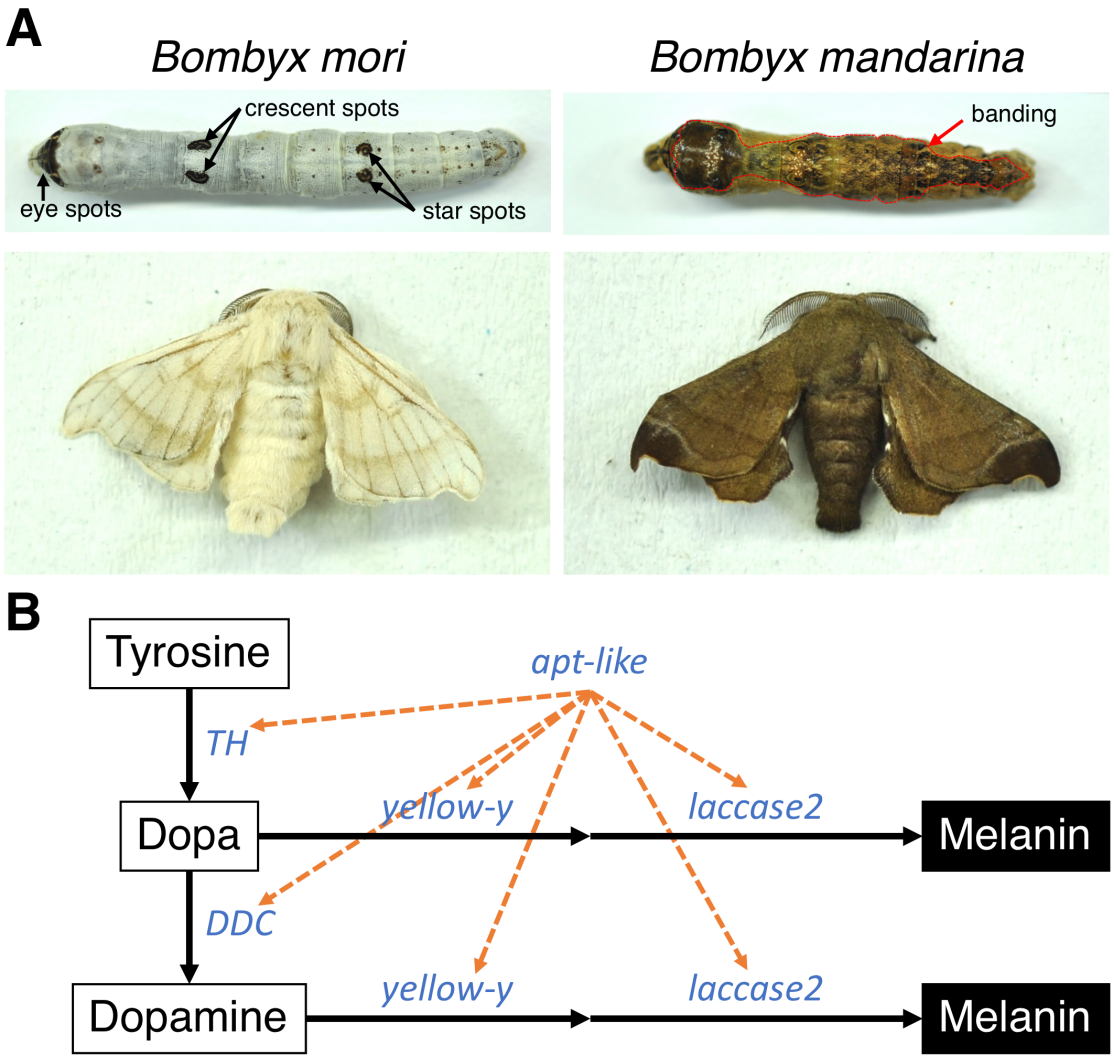

552

553 **Figure 1.** (A) Larvae (top) and adult males (bottom) of *B. mori* (left) and *B. mandarina*
554 (right). Black arrows indicate larval spot markings (eye spots, crescent spots and star
555 spots) and red dotted lines delimit the larval dorsal pigment patterning ("banding").
556 The names of spots follow the nomenclature of Yoda *et al.* (2014). (B) The proposed
557 melanin biosynthesis pathway in *Bombyx* larvae largely adapted from Futahashi *et al.*
558 (2008) and Yoda *et al.* (2014). Orange dashed arrows indicate presumed regulation of
559 genes by the transcription factor *apt-like*.

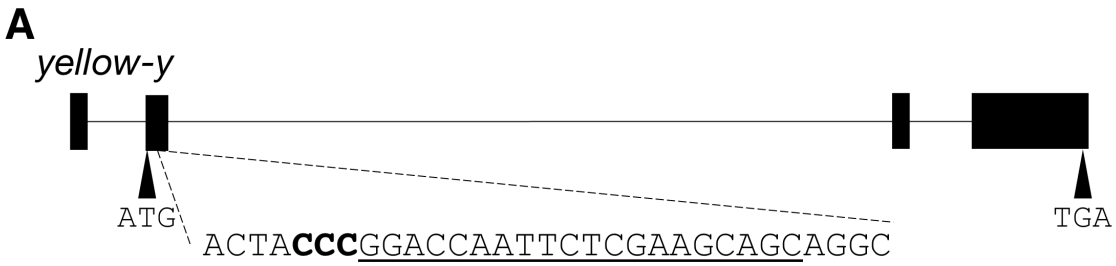

B

	Trp	**Asn**	**Tyr**	**Pro**	**Asp**	**Gln**	**Phe**	**Ser**	**Lys**	**Gln**	**Gln**	**Ala**	**Leu**	**Arg**	**Thr**	**Gly**
Wild type	TGG	AAC	TA**C**	**CC**G	GAC	CAG	TTC	TCG	AAG	CAG	CAG	GCT	CTC	AGG	ACT	GGT
yellow-y$^{\Delta 5}$	TGG	AAC	TAC	CC-	---	--	-AA	TTC	TCG	AAG	CAG	CAG	GCT	CTC	AGG	ACT	GGT

Figure 2. The nature of the lesion in the *yellow-y* knockout (*yellow-y*$^{\Delta 5}$) in *B. mandarina*. (A) Gene structure of *yellow-y* and the selected crRNA target site. The target sequence is underlined and the protospacer adjacent motif (PAM) site is shown in bold letters. (B) Alignment of the *yellow-y* gene sequences surrounding the crRNA target site from wild type, and G_2 *B. mandarina* individuals that are homozygous for a 5-base pair deletion and associated single nucleotide mutation. The target sequence is underlined, and the PAM site (CCN) is indicated in bold letters.

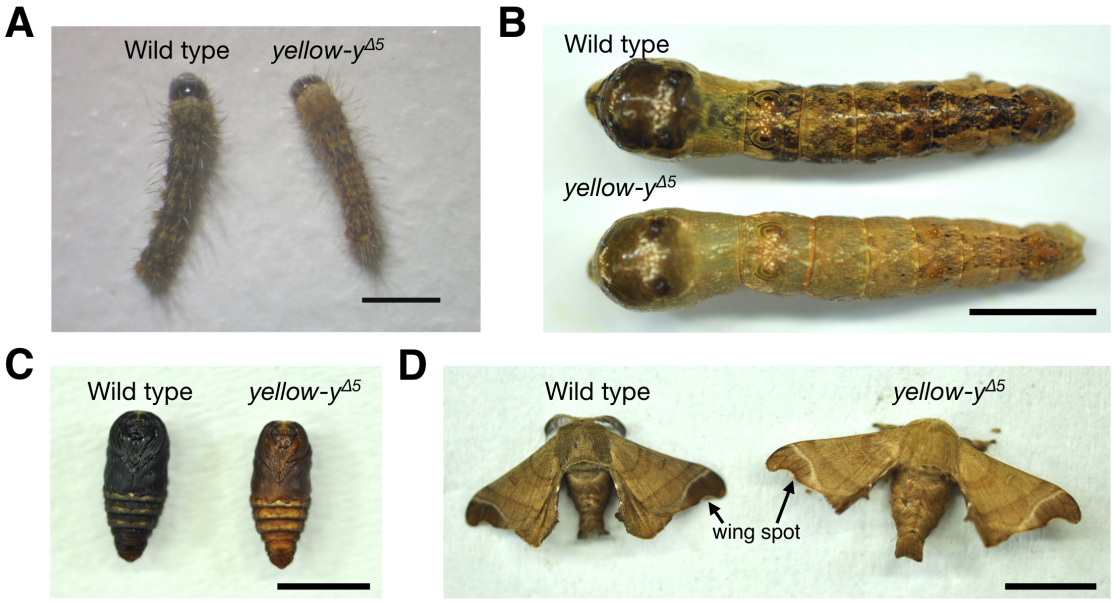

569

570 **Figure 3.** The phenotypes of wild-type and *yellow-y* knockout mutants of *B. mandarina*.

571 Representative (A) neonate larvae, (B) final-instar larvae, (C) male pupae and (D) adult

572 male moths of wild-type (left or top) and *yellow-y*$^{\Delta 5}$ (right or bottom) *B. mandarina*.

573 Arrows indicate wing spot markings in adult moths. Scale bars: 1 mm (A) or 1 cm (B-

574 D).

575

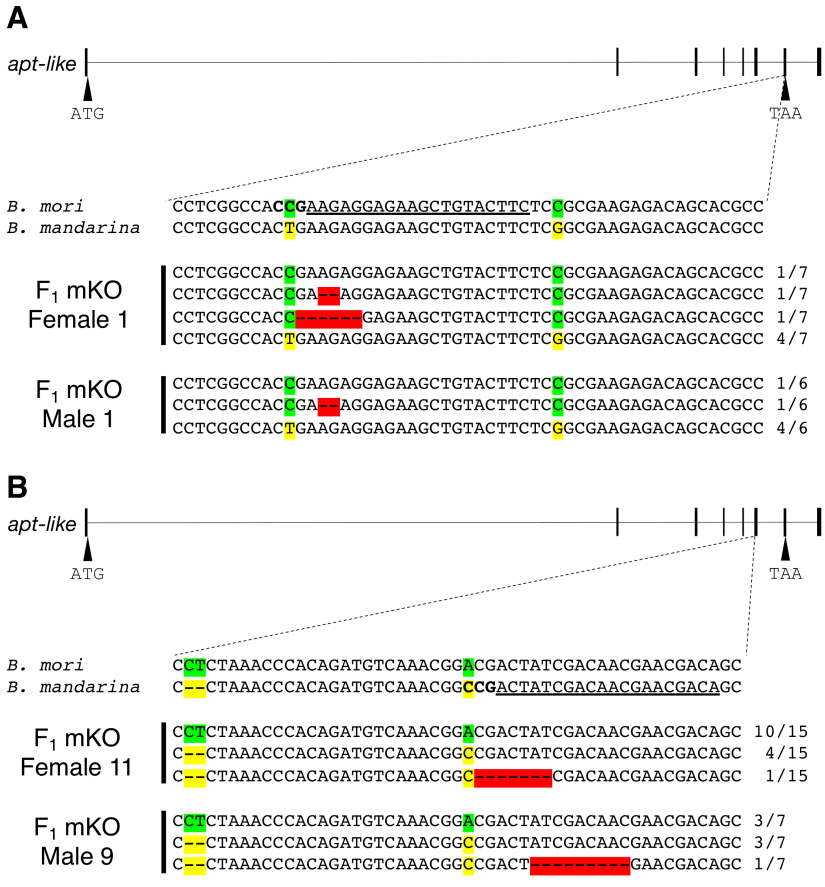

Figure 4. Mutations introduced by *allele-specific apt-like* mosaic knockout (mKO) in F_1 hybrids. Annotation and inset alignments of the *apt-like* gene in both species with selected crRNA target sites whose PAM sequences are only present in (A) *B. mori* or (B) *B. mandarina*. Two *allele-specific* knockout individuals were sequenced for each target. The target sequences are underlined, and the PAM sequences are shown in bold letters. *B. mori* specific SNPs and *B. mandarina* specific single nucleotide variants are highlighted with green and yellow shadings, respectively. Mutations introduced by CRISPR/Cas9 system are highlighted with red shading. Numbers on the right edge indicate the numbers of the clones identified among all cloned and sequenced PCR products.

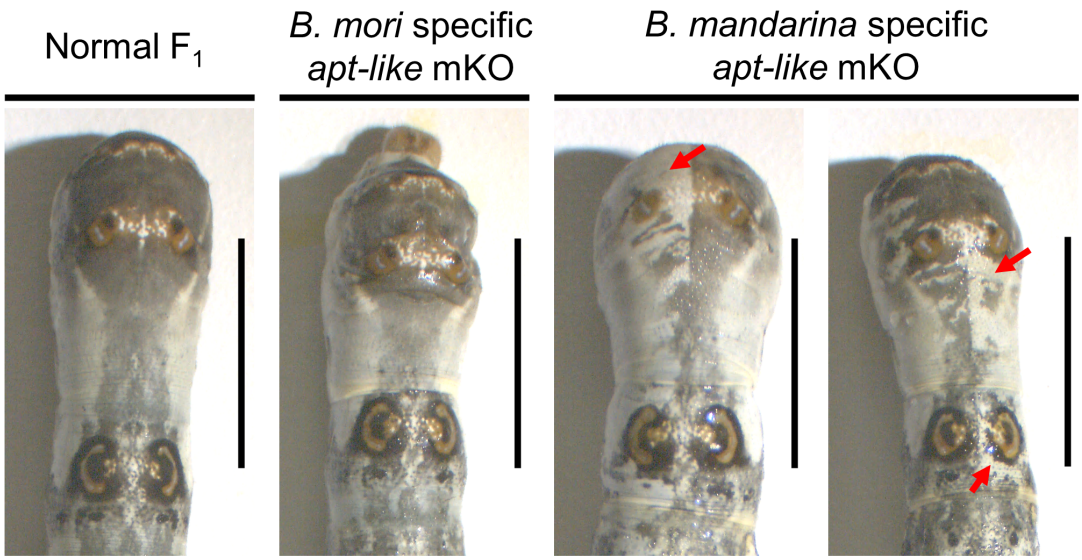

587

588 **Figure 5.** Representative fifth instar larvae of normal F_1 (left), *allele-specific apt-like*

589 mKOs targeting the *B. mori* allele (middle) and the *B. mandarina* allele (right). Red

590 arrows indicate ectopic white (depigmented) regions. Scale bars: 1 cm.

591

592 **Table S1** PCR primers and RNA sequences used in this study.

Primer Name	Sequence	Usage
PCR primers		
yellow-y_cloning_F02	AAGCTGCCGCGAACATAG	RT-PCR and CDS cloning
yellow-y_cloning_R02	TGCAATAGAAAGCCTCACATTT	RT-PCR and CDS cloning
apt-like_cloning_F	GAAAATAAGAGCCCACGCACT	RT-PCR and CDS cloning
apt-like_cloning_R	ACTTGAATCCGCTTTTGACG	RT-PCR and CDS cloning
yellow-y_mid_F	CGTCTTTGGGTATTAGACGTTGG	CDS cloning
yellow_y_check_F	GTACATACCTGAGCGCCACCT	Genomic PCR for mutation detection and sequencing in CRISPR/Cas9-targeted gene knockout
yellow_y_check_R	CAGCAACGATAAAGCTCCAAG	Genomic PCR for mutation detection and sequencing in CRISPR/Cas9-targeted gene knockout
Bmand_apt-like_F03	GAGGTTTTGTGTGGCGAGATG	Genomic PCR for mutation detection and sequencing in CRISPR/Cas9-targeted gene knockout
Bmand_apt-like_R02	AGGAAGTTCTGCTGGAGTCTG	Genomic PCR for mutation detection and sequencing in CRISPR/Cas9-targeted gene knockout
Bmori_apt-like_F01	CTGGACGATCACATAAAGCAC	Genomic PCR for mutation detection and sequencing in CRISPR/Cas9-targeted gene knockout
Bmori_apt-like_R01	TCTCAACTCAATGAGGAACAGC	Genomic PCR for mutation detection and sequencing in CRISPR/Cas9-targeted gene knockout
RNAs		
yellow-y_crRNA_1	GCUGCUUCGAGAAUUGGUCCGUUUUAGAGCUAUGCUGUUUUG	CRISPR/Cas9-targeted gene knockout
Bmori_apt-like_specific_crRNA	GAAGUACAGCUUCUCCUCUUGUUUUAGAGCUAUGCUGUUUUG	CRISPR/Cas9-targeted gene knockout
Bmand_apt-like_specific_crRNA	UGUCGUUCGUUGUCGAUAGUGUUUUAGAGCUAUGCUGUUUUG	CRISPR/Cas9-targeted gene knockout
tracrRNA	AAACAGCAUAGCAAGUUAAAAUAAGGCUAGUCCGUUAUCAACUUGAAAAAGUGGCACCGAGUCGGUGCUUUUUUU	CRISPR/Cas9-targeted gene knockout

593

594

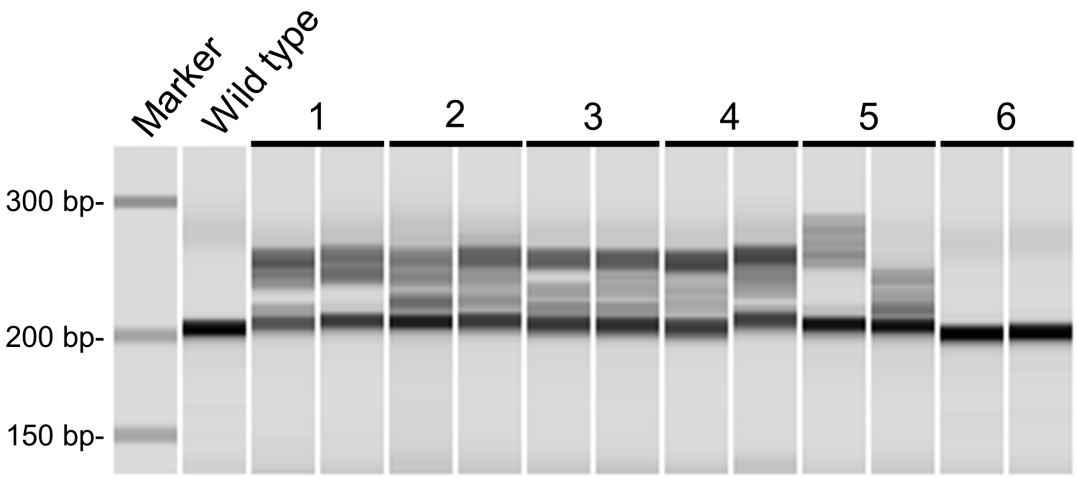

595

596 **Figure S1.** Detection of mutations at the *yellow-y* crRNA target site using a heteroduplex
597 mobility shift assay. Two intervals were prepared for each G_1 brood. Ten eggs were
598 collected into one tube, and genomic DNA was prepared. The region containing the
599 target site of *yellow-y* crRNA was PCR-amplified. Multiple heteroduplex bands caused
600 by insertion/deletion mismatches were observed indicating the presence of DNA lesions
601 (insertions/deletions and/or associated nucleotide variants).

602

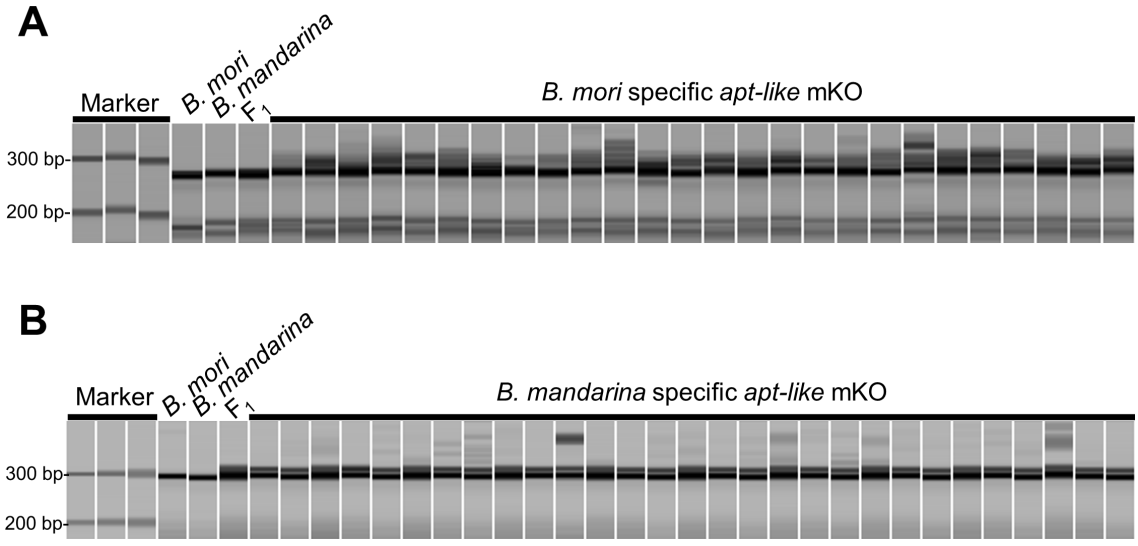

603

604

605 **Figure S2.** Detection of mutations at *apt-like* crRNA target sites using a heteroduplex

606 mobility shift assay. The region containing the target site of (A) *B. mori* specific *apt-*

607 *like* crRNA and (B) *B. mandarina* specific *apt-like* crRNA was PCR-amplified using

608 DNA prepared from G_0 adults' legs. Multiple heteroduplex bands caused by

609 insertion/deletion mismatches and associated nucleotide variants were observed in G_0

610 mosaics.

611

612

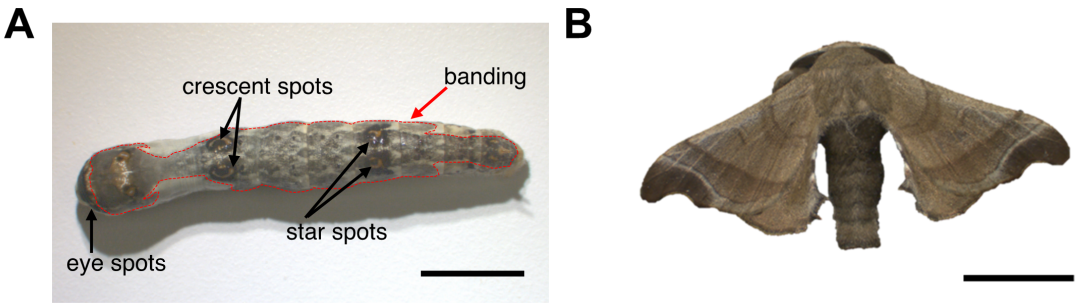

Figure S3. A representative (A) fifth instar larva and (B) adult male moth of normal F_1 (*B mori* female × *B. mandarina* male). Black arrows indicate larval spot markings and red dotted lines outline the banding. Normal F_1 larvae have a dark body with darker greyish brown banding covering wide range of the dorsal surface similar to *B. mandarina*. The names of spots were referred to Yoda *et al.* (2014). Scale bars: 1 cm.

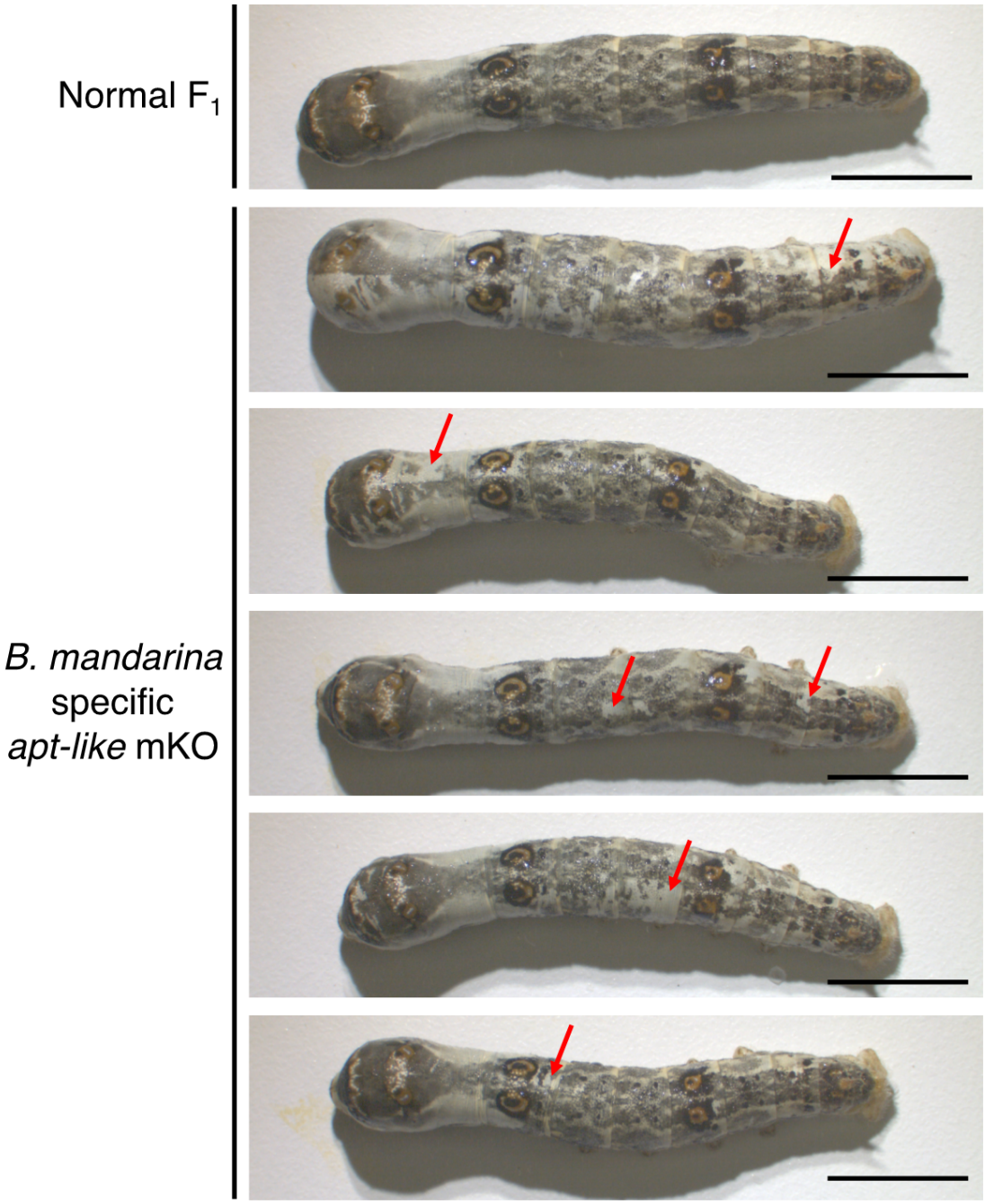

620

621 **Figure S4.** Fifth instar larvae of normal F_1 and *B. mandarina* specific *apt-like* mKO.

622 Red arrows indicate ectopic white (depigmented) regions. Crescent and star spots were

623 not depigmented in all larvae. Scale bars: 1 cm.